2016
International Symposium on Power Electronics,
Electrical Drives, Automation and Motion

Design of a High-Power Multilevel Chopper with 1700 V / 300 A SiC MOSFET Half-Bridge Modules

Joseph Fabre, Philippe Ladoux, *Member, IEEE*
LAPLACE, Université de Toulouse, CNRS, INPT, UPS, France
2 rue Charles Camichel - BP 7122
F-31071 Toulouse, France
Joseph.Fabre@laplace.univ-tlse.fr
Philippe.Ladoux@laplace.univ-tlse.fr

***Abstract*—Silicon (Si) IGBTs are widely used in power converters. Silicon Carbide (SiC) technology will push the limits of switching devices in three directions: higher blocking voltage, higher operating temperature and higher switching speed. The first SiC-MOSFET Half-Bridge Modules (SiC-MOSFET HBMs) are now commercially available and look promising. Although they are still limited in breakdown voltage, these components should, for instance, improve conversion efficiencies. In particular, a significant reduction in switching losses is to be expected which should lead to improvements in power-to-weight ratios. Nevertheless, because of the high switching speed and the high current levels required by high-power applications, the implementation of these modules is critical. In this paper, the authors investigate the design of a particular structure, called Imbricated Cells Multilevel Chopper (ICMC) or else Flying Capacitor Converter and this with 1700 V/300 A SiC-MOSFET HBMs. The reactive components forming this converter, such as the flying-capacitors, are dimensioned. The characteristics of this converter are calculated, plotted, and compared to the same structure with 1700 V / 300 A Si-IGBT Modules.**

***Index Terms*—Multilevel systems, DC-DC power converters, Choppers (circuits), Loss measurement, Power MOSFET, Power semiconductor devices, Silicon carbide, Wide band gap semiconductors.**

I. INTRODUCTION

Power electronics has historically used silicon semiconductors. For example, IGBTs (Insulated-Gate Bipolar Transistors) arrived in railway traction converters in 1992 [1] and quickly supplanted bipolar devices such as phase-controlled thyristors or GTOs (Gate Turn-Off Thyristors). While improvements continue to be made [2], silicon technology is reaching an asymptote and progress on breakdown-voltage and switching performance is limited.

Recently, some semiconductor manufacturers began the production of SiC transistors with breakdown voltages of 1200 V or even 1700 V [3-5]. For ten years, many publications showed that SiC devices are very attractive in terms of blocking voltage [6], operating temperature [7] and switching frequency [8] which is why many power converter manufacturers now have to seriously consider this new technology [9], [10]. The first commercial SiC-MOSFET HBMs essentially push the limits of switching speeds and allow an increase in converter efficiency.

To evaluate the potential of these new devices, the authors achieved many test-benches, which are presented in these papers [11-12]. Now, the authors propose to study the contribution of SiC-MOSFET HBM to a particular structure, called Imbricated Cells Multilevel Chopper (ICMC) or else Flying Capacitor Converter.

The ICMC and more generally the concept of multilevel converters have been introduced in the 90's [13-17]. In the recent years, the increasing market of high-power converter and the difficulty to maintain good performance of the semiconductor when the voltage rating increases, demonstrate more and more the usefulness of this structure. In high-voltage DC to DC conversion, the ICMC allows distributing the voltage between semiconductors in series through floating capacitors. This voltage distribution allows for using switching devices of smaller rating voltage and more efficient, and also improves the output waveform quality.

In this paper, the authors study the design of a DC-DC converter with an input voltage of 3500 V and an output voltage of 1550 V. To build this converter, 1700 V/300 A SiC-MOSFET HBMs are used. These wide band gap components are compared to Si-IGBT modules of same voltage and current ratings. Such study aims to show the advantages of SiC devices for the design of ICMCs.

II. NUMBER OF IMBRICATED CELLS

The general topology of ICMC is shown in Fig.1. Where n is the number of imbricated commutation cells. We assume that capacitors values $C_{f\,k}$ (k = *[1, 2, ..., n]*) are sufficient to keep the voltage $V_{Cf\,k}$ constant with the following distribution [16]:

$$V_{Cfk} = \frac{k \times V_{in}}{n} \; ; \; k = [1,2,..., n] \qquad (1)$$

The voltage distribution on these capacitors allows limiting the maximum voltage on each semiconductor to V_{in} /n. The elementary commutation cells are shows in Fig.1, for

978-1-5090-2067-6/16/$31.00 ©2016 IEEE

example, the pairs T_{r1} and D_1 (cell 1), or Tr_n and D_n (cell n), operate with a voltage V_{in}/n and switch output current Io.

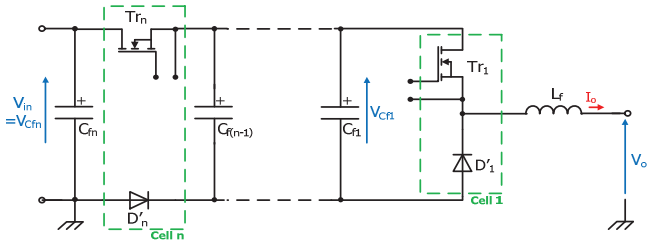

Fig. 1. Topology of Imbricated Cells Multilevel Chopper (ICMC).

In our application, considering SiC-MOSFET HBM, an internal connection exists between the top and bottom switch, making it suitable for cell 1, but not for the other cells. HBM will not be used with two complementary switches but with two independent switches, for example, to achieve the function: $Tr_{(k-1)}$ and Tr_k. This particular use of HBM is an unusual constraint for the thermal stress because the two switches of the package can operate simultaneously. On the other hand, from an intrinsic design point of view, insulation between the drain of the higher switch and the source of the bottom switch is only the rated voltage of the switch (1700 V in our case). This leads to the following inequation, where V_{n_pack} is the HBM voltage rating:

$$\left[\left(V_{Cfk} - V_{Cf\,(k-2)}\right) = \frac{2.V_{in}}{n}\right] \leq V_{n\_pack} \qquad (2)$$

To size our converter, using equation (1) and considering 1700 V semiconductors, four cells seem appropriated since each switch operates at : 3500 / 4 = 875 V. This may be satisfactory with 1700 V single switches, but with HBMs, inequation (2) is not satisfied since $(V_{Cf\,k} - V_{Cf\,(k-2)})$ = 1750 V and $V_{n\ pack}$ = 1700 V. In order to satisfy inequation (2), the converter should have five HBMs. Fig. 2 shows the ICMC, with five 1700 V/300 A SiC-MOSFET HBMs.

The switching loop A, composed by HBM n°3 (cell 1) and capacitor C_{f1}, is classic and requires a complementary control of the switches. In contrast, the other loops are composed of two capacitors and two different HBMs. However, the main advantage of SiC devices comes from their high switching-speed, a special care should be taken in circuit layout to minimize the loop-inductance (capacitors, bus-bar and SiC-MOSFET HBM) [18-21]. The connections to the flying capacitors have to be considered with regards to high-speed switching and high-current capability. This is important to minimize voltage transients due to the high turn-off di/dt, which could destroy the semiconductor device even if the elementary commutation cell operates at 700 V.

III. Estimation of Losses – Comparison of SiC-MOSFET HBM Versus Si-IGBT HBM

In this section 1700 V/300 A SiC-MOSFET HBMs performances are compared with Si-IGBT modules of the same caliber and the same packaging.

A. Conduction characteristics comparison

I-V characteristics of the two devices were obtained for the maximum junction temperature: T_j = 150 °C. Fig. 3 (a) shows the transistor on-state characteristics of both and it can be seen that the MOSFET has lower forward voltage drop at 100 A. Fig. 3 (b) shows the diode forward characteristics. The SiC-MOSFET in parallel to the SiC-SBD (Schottky Barrier Diode) can operate with a reverse current especially thanks to its channel, whose opening is related to the gate-source voltage V_{gs}. Thus, when the gate voltage V_{gs} = -5 V (blue curve), the channel is completely closed ($V_{gs} < V_{gsTH}$) and when V_{gs} = 20 V (green curve), the channel is opened and the reverse current is divided between the transistor and the antiparallel SBD. This particular property of the MOSFET can be used to reduce losses on all the bottom switches of our converter ($Tr'_{[1\text{-}5]}$ and $D'_{[1\text{-}5]}$ in Fig. 2).

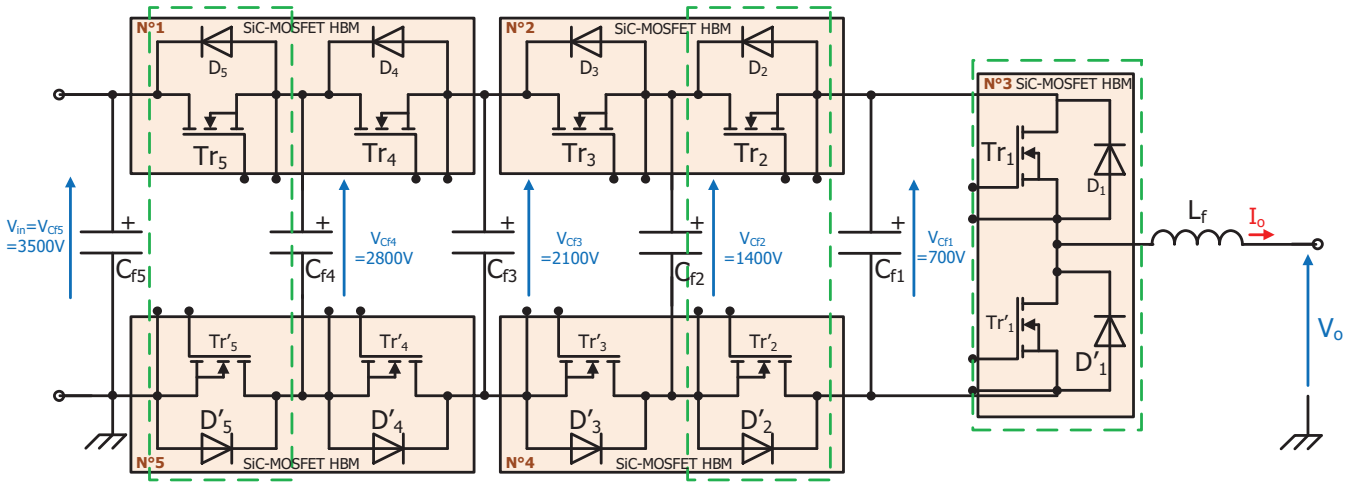

Fig. 2. Topology of a multilevel chopper, with five imbricated cells, and based on 1700 V / 300 A SiC-MOSFET HBMs.

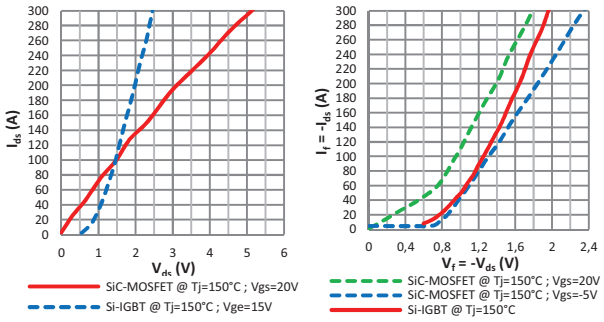

(a) (b)

Fig. 3. (a) $I_{ds} = f(V_{ds})$ - transistor on-state characteristics, (b) $I_f = f(V_f)$ - diode forward characteristics.

B. *Switching characteristics comparison*

As shown in Fig. 4, the switching energies of the SiC-MOSFET HBM are dramatically lower than those of the equivalent Si-IGBT module. At 300 A and for T_j = 150°C, the reduction factor is about 9 at turn-off and about 6 at turn-on; the recovery energy of the SiC-SBD is about 67 times lower than that of the Si-PiN diode.

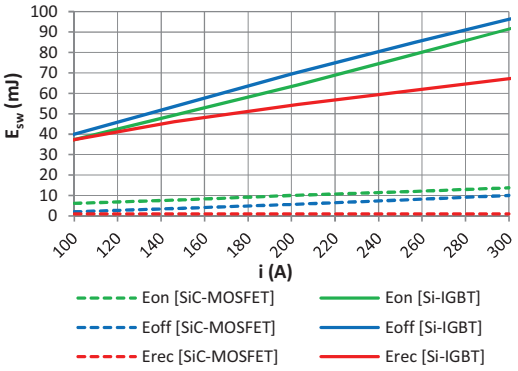

Conditions:
Si-IGBT: V_{ge} = ±15 V, $R_{Gon} = R_{Goff}$ = 2.4 Ω, V_{CE} = 900 V.
SiC-MOSFET: V_{gs} = -5/+20 V, $R_{Gon} = R_{Goff}$ = 2.5 Ω, V_{DS} = 900 V.

Fig. 4. Switching losses versus commutated current at T_j = 150°C. Comparison between 1700 V / 300 A SiC-MOSFET HBM and Si-IGBT with same rating.

C. *Semiconductor losses in the ICMC*

Losses are calculated by using all parameters extracted from the curves in Fig. 3 and Fig. 4, and for one junction temperature.

Equation (3) is used to calculate the transistor losses:

$$P_{Tr} = (V_{0T} \times \alpha \times I_o) + (r_{dT} \times \alpha \times I_o^{\,2}) + \frac{V_{DC}}{V_{ref}} \times f_{sw} \times \left\{ \begin{array}{l} [(a_{ON} \times I_o^{\,2}) + (b_{ON} \times I_o) + c_{ON}] \\ + [(a_{OFF} \times I_o^{\,2}) + (b_{OFF} \times I_o) + c_{OFF}] \end{array} \right\} \quad (3)$$

Equation (4) is used to calculate the diode losses:

$$P_D = (V_{0D} \times (1-\alpha) \times I_o) + (r_{dD} \times (1-\alpha) \times I_o^{\,2}) + \frac{V_{DC}}{V_{ref}} \times f_{sw} \times [(a_{REC} \times I_o^{\,2}) + (b_{REC} \times I_o) + c_{REC}] \quad (4)$$

Where:

V_0, r_d: conduction parameters;
a, b, c : parameters of interpolated curves for switching energy;
α: duty cycle;
V_{DC}: voltage in each switching cell (700 V);
V_{ref}: voltage reference for switching energy (900 V);
f_{sw}: switching frequency;
I_o: output current, considered as constant.

Thus, power losses in the ICMC can be calculated for several output current values I_o and several switching frequencies f_{sw}. Table I shows power losses for an operating point of the ICMC. Compared to Si-IGBT modules, SiC-MOSFET HBMs allow an overall loss reduction of over 75%. Moreover, the reduction is even greater (over 77%) if bottom MOSFETs ($Tr'_{[1\text{-}5]}$) are used in reverse conduction mode.

TABLE I
POWER LOSS COMPARISON OF ICMC: SIC-MOSFET VERSUS SI-IGBT

V_{switch} = 700 V I_o = 100 A T_j = 150°C f_{sw} = 10 kHz α_{max} = 0.6		Si-IGBT	SiC-MOSFET	
			no-reverse current in $Tr'_{[1\text{-}5]}$	reverse current in $Tr'_{[1\text{-}5]}$
P_{cond} (W)	$Tr_{[1\text{-}5]}$	87.4	101.1	101.1
	$D_{[1\text{-}5]}$	0.0	0.0	0.0
	$Tr'_{[1\text{-}5]}$	0.0	0.0	39.1
	$D'_{[1\text{-}5]}$	76.2	81.1	20.3
P_{sw} (W)	$Tr_{[1\text{-}5]}$	593.4	63.1	63.1
	$D_{[1\text{-}5]}$	0.0	0.0	0.0
	$Tr'_{[1\text{-}5]}$	0.0	0.0	0.0
	$D'_{[1\text{-}5]}$	268.8	7.8	7.8
P_{cond} + P_{sw} (W)	$Tr_{[1\text{-}5]}$	680.8	164.3	164.3
	$D_{[1\text{-}5]}$	0.0	0.0	0.0
	$Tr'_{[1\text{-}5]}$	0.0	0.0	39.1
	$D'_{[1\text{-}5]}$	345.0	88.9	28.0
Total power losses in the ICMC (W)		5129.0	1266.0	1157.0
Losses reduction (%) $[(P_{SiC} / P_{Si} - 1).100]$			-75.3	-77.4

D. *Thermal limits and choice of the cooling system*

Once the losses on each module are calculated, the choice of the cooling system can be performed. The thermal model presented in Fig. 5 is used. The following assumptions are considered: the maximum junction temperature is 150°C, the maximum case temperature is 125°C and the maximum ambient temperature is 40°C.

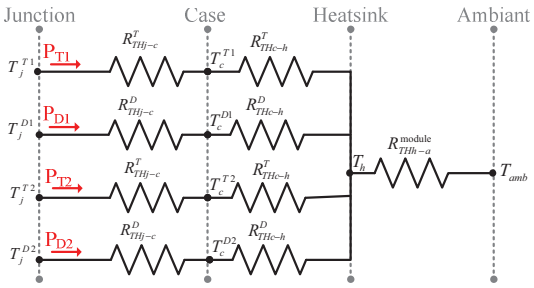

Fig. 5. Thermal model for each HBM.

Fig. 6 shows the calculation results for the most thermally constrained HBMs (No.1 or No.2 in Fig. 2). For the cooling system, two different technologies are compared: one with forced air ($R_{THh\text{-}a}$ = 150°C/kW) and the other with water circulation ($R_{THh\text{-}a}$ = 20°C/kW). These curves highlight the advantage of SiC-MOSFET compared to Si-IGBT. Considering an air-cooling system and a switching frequency of 10 kHz, the thermal limit is reached for Si-IGBT HBMs with an output current at 20 A, whereas 130 A can be delivered with SiC-MOSFET HBMs. The difference is even greater with a water cooling system. Si-IGBTs can operate up to 100 A whereas SiC-MOSFETs allow to supply 240 A. Another noticeable interest in Fig. 6 is to show the possibility to increase the switching frequency of SiC-MOSFETs. As example, with a water cooling system, SiC-MOSFETs can operate at 50 kHz with an output current at 160 A, while this is not possible with Si-IGBTs.

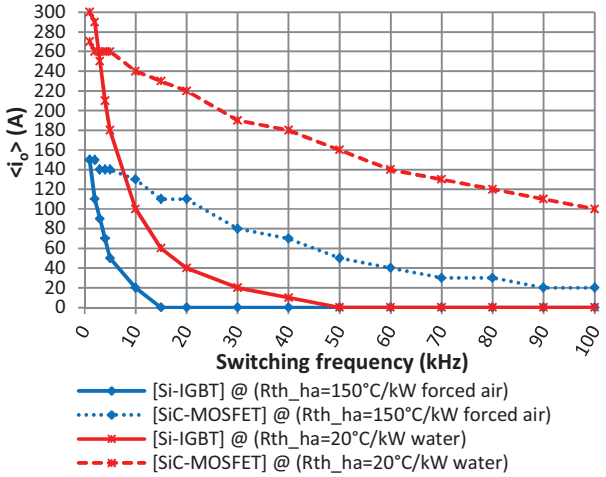

Fig. 6. ICMC maximum output current versus switching frequency considering two technologies of cooling system.

To take full advantage of these power modules, the best water cooling system is selected. Each HBM is mounted on an individual cold plate with a heat transfer coefficient $H_{h\text{-}a}$ = 7653 $W.m^{-2}.°C^{-1}$ and a thermal resistance $R_{THh\text{-}a}$ = 20 °C/kW, at a water flow rate Q_v = 5 L/min (Fig. 7). This solution is more compact than the forced air one, thereby facilitating the implementation of the entire converter.

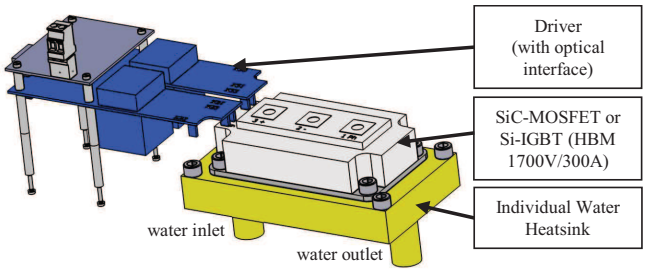

Fig. 7. Design of SiC-MOSFET HBM with individual liquid cold plate and individual driver.

To highlight the interest of SiC-MOSFET HBMs, the efficiency of ICMC can be calculated for several output currents and switching frequencies, while showing the thermal limits. Fig. 8 shows an example of efficiency calculations according to the converter output current (losses in flying capacitors are neglected). Two switching frequencies were considered: Fig.8 (a) with f_{sw} = 10 kHz and Fig.8 (b) with f_{sw} = 50 kHz. Fig. 9 shows efficiency according to switching frequency, for a fixed output current I_o = 100 A. For a switching frequency at 1 kHz, the Si-IGBT solution with an efficiency of 98.95% is better than the SiC-MOSFET solution which reaches only 98.78%. In contrast, when the switching frequency increases, the efficiency of the Si-IGBT solution decreases rapidly to 96.8% while the thermal limit is reached at 10 kHz. For the same switching frequency, SiC-MOSFETs allow maintaining good performances for the converter with 98.73% efficiency. As a result, the switching frequency can be sensibly increased up to 50 kHz. At this operating point (I_o = 100 A), the efficiency is still 98.22%, and the thermal limit is not yet reached.

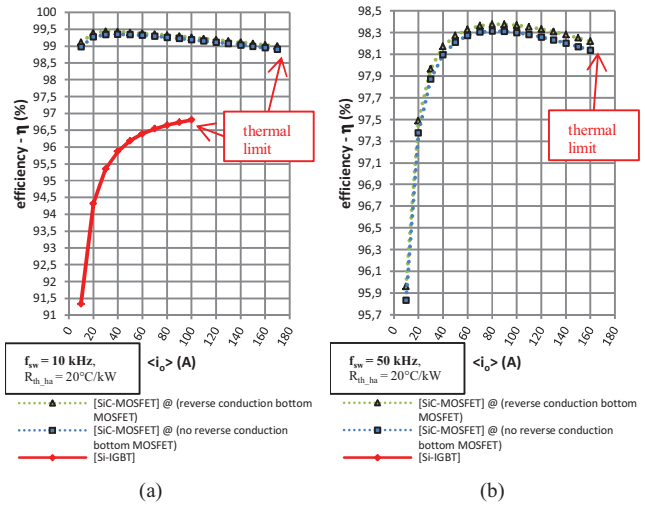

(a) (b)

Fig. 8. ICMC power efficiency - Comparison between 1700 V / 300 A SiC-MOSFET HBM and Si-IGBT with same rating – (a) at f_{sw} = *10 kHz*, (b) at f_{sw} = *50 kHz*.

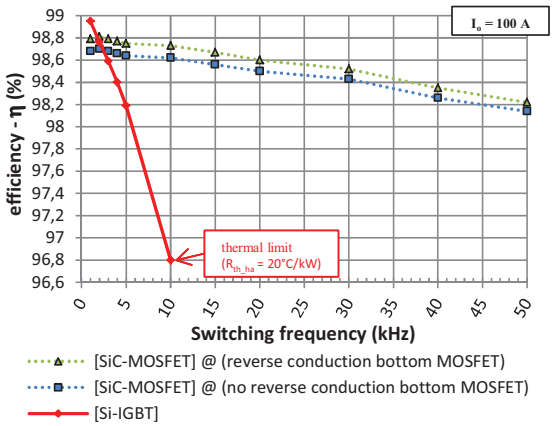

Fig. 9. ICMC power efficiency versus switching frequency- Comparison between 1700 V / 300 A SiC-MOSFET HBM and equivalent Si-IGBT.

In this section, the interest of SiC-MOSFET HBMs in terms of efficiency has been demonstrated. Nevertheless, the increase of the switching frequency has to be considered in the design of the multilevel converter.

IV. Experimental Setup - Design of the Set: Flying Capacitors / Bus-bars / HBM

A. Choice of flying capacitors

In the following study we assumed that the current ripple in the output inductor L_f is neglected. The value of the flying capacitors C_{fk}, is determined through equation (5) originating from the reference [14].

$$C_{fk} \geq \frac{I_o}{n \,.\, f_{sw} \,.\, \Delta V_{Cfk\,\max}} \tag{5}$$

The value of the capacitor is calculated considering that maximum voltage ripple $\Delta V_{Cf\_k\_max}$, is fixed at 25% of the commutation cell voltage equal to $\frac{V_{in}}{n}$. Otherwise, the RMS current in each flying capacitor is given by:

$$I_{Cfk\_RMS} = \sqrt{\frac{2}{n}} \times I_o \tag{6}$$

According to (5) and (6), the minimum capacitance values and the corresponding RMS current are reported in Fig. 10 where the operating limits, already presented in Fig. 6, are plotted. For I_o = 100 A, the RMS value of the current in each flying capacitor is 63.5A. With Si-IGBTs the maximum switching frequency is 10 kHz which gives a minimum value of the flying capacitors at 11.5 µF. Likewise, with SiC-MOSFETs, the switching frequency can be increased to 100 kHz, which leads to a capacitance ten times lower, but with the same RMS current value. Thus, the theoretical benefit introduced by the increase of the switching frequency on the value of the floating capacitors is minimized by the fact that the RMS current is always the same.

From a technological point of view, the capacitors must have a low capacitance but with a high breakdown voltage and a high RMS current. Moreover, it should be noted that SiC-MOSFETs requires a very low inductance in the commutation mesh which includes the capacitors, the bus-bar and the package of the HBMs. In practice, it is not so easy to find a capacitor with a very low series inductance. One possibility is to work with the capacitor manufacturer in order to get specific capacitors which meet SiC-MOSFET HBM requirements. The other possibility, in the short-term, is to use existing capacitors. The design of the ICMC proposed in this paper allows complying with constraints of compactness and implementation and is able to operate at the maximum output current over a wide switching frequency range. Our selection was performed on the capacitors "FFVS" (a range of capacitors with low inductance for power electronics) proposed by manufacturer AVX [22]. The same reference is used for the entire converter, with: V_n = 1900 V, C = 14 µF, I_{rms} = 66A, L = 10nH, *Volume* = 520 cm^3 and *Weight* = 345 g.

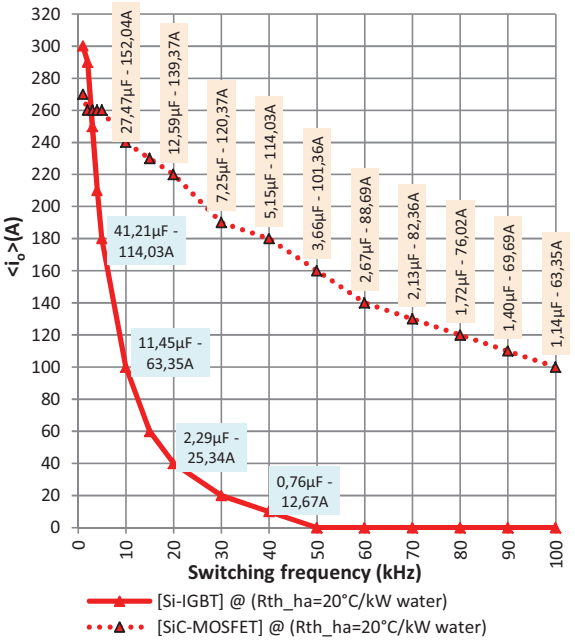

Fig. 10. Flying capacitor value and corresponding RMS current for each operating points presented in Fig.6.

Table II outlines the arrangements required for each floating capacitor of the ICMC. Fig. 11 shows the output current capability resulting from this choice of capacitors. Obviously, as it was shown in Fig. 10, if the operation is limited to SiC-MOSFETs with a switching frequency at 100 kHz, capacitors would be less bulky and lighter.

However, our ICMC is designed to compare the performance of Si-IGBTs and SiC-MOSFETs and is able to work on a wide frequency range. According to Fig. 11, with a switching frequency at 10 kHz, it allows to operate at a maximum output current of 100 A with Si-IGBT HBMs and 180 A with SiC-MOSFET HBMs. On the other hand, SiC-MOSFET HBMs are able to switch at 50 kHz with an output current at 160 A, while the efficiency of the ICMC, of about 98%, is still satisfactory.

TABLE II
EXAMPLE CHOICE OF FLOATING CAPACITORS FOR THE ICMC

	C_{f1}	C_{f2}	C_{f3}	C_{f4}	C_{f5}
$V_{Cf\,n}$ (V)	700	1400	2100	2800	3500
$V_{Cf\,max}$ (V)	788	1488	2188	2888	3588
Topology (series / parallels)					
$C_{f\,total}$ (µF)	42	42	21	21	21
I_{RMS} (A)	198	198	198	198	198
$L_{theoretical}$ (nH)	3.3	3.3	6.7	6.7	6.7
Total vol. and weight	0.13 m^3 / 8.28 kg				

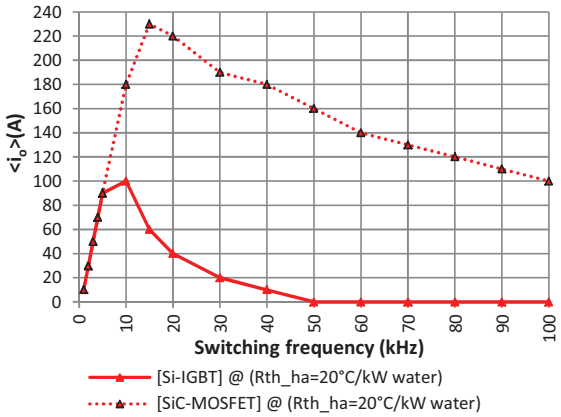

Fig. 11. Performances of the ICMC after sizing of flying capacitors.

B. *Design of the set of ICMC converter: Flying Capacitors / Bus-bars connection / HBMs / Drivers*

To assist in the design of the ICMC, an innovative procedure was adopted, based on 3D electromagnetic modeling. This co-simulation allowed a complete modeling of the electrical behavior of the flying capacitors / laminated bus-bar connections / HBMs / driver circuits [12] in order to determine the optimal position of the components which minimizes the loop inductances. For that, a mechanical design of the entire ICMC was performed with *Autodesk_Inventor* software. Then, a co-simulation with *Q3D* and *Simplorer* allowed taking into account all the assembly elements [18-21]. Fig. 11 shows the final 3-D design and Table III shows the loop-inductance values given by the co-simulation results. The proposed layout leads to a fairly low loop-inductance value, with 132 nH in the worst case (loop E), what is acceptable given the turn-off *di/dt* of the SiC devices.

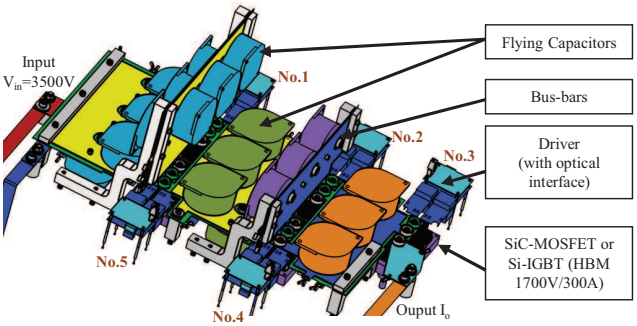

Fig. 11. 3D design of the ICMC converter (Flying Capacitors / Bus-bars / HBM / Drivers).

TABLE III
RESULTS OF CO-SIMULATION STUDY - ESTIMATION OF PARASITIC LOOP-INDUCTANCE (FLYING CAPACITORS / BUS-BARS CONNECTION / HBMS)

(measured at 1 kHz)	L_{loop} (nH)
Loop A (C_{f1} - Tr_1 - D'_1)	38
Loop B (C_{f1} - C_{f2} - Tr_2 - D'_2)	102
Loop C (C_{f2} - C_{f3} - Tr_3 - D'_3)	123
Loop D (C_{f3} - C_{f4} - Tr_4 - D'_4)	131
Loop E (C_{f4} - C_{f5} - Tr_5 - D'_5)	132

All in all, the design of the set (flying capacitors / laminated bus-bar connections / HBMs / driver circuits) is not easy. The theoretical expected gain on floating capacitor, when the switching frequency increases, is not evident in practice. Indeed, it is necessary to use specific capacitors having a low capacitance value, a high breakdown voltage and a high RMS current rating. Moreover, these capacitors should have a suitable geometry which facilitates the implantation in the ICMC while minimizing the loop inductances. Nevertheless, simulations performed with a 3D model have shown that it is already possible to take advantage of SiC devices even though classical housing of capacitors and HBMs are still used.

C. *Electrical insulation in the choice of assembly elements*

The insulation for a high voltage structure requires the use of specific devices. It is important to take this into account when designing. In our assembling, this insulation has been set at 8 kVrms (at 50 Hz, during 1 min).

To fulfill this constraint, specific DC/DC converters [23] were developed to supply the gate drivers. Moreover, the voltage and current sensors used for the control of the converter are from the manufacturer LEM [24] and chosen in the series LV or DV. In addition, all the control of the SiC-MOSFET is effective by optic fiber. Besides insulation it helps to limit EMC problems caused by the fast switching of SiC-MOSFETs.

In the cooling system, the length of the water pipes is also chosen to provide a sufficient insulation between two adjoining cold plates.

Fig. 12 shows the final 3-D design of the ICMC converter prototype and one picture of the real test-bench.

V. CONCLUSION

In this paper, the authors presented the design of a multilevel chopper based on five 1700 V/300 A HBMs. The sizing was performed considering Si-IGBTs and SiC-MOSFETs.

With SiC-MOSFET devices, it was shown that the switching frequency can be increase to 50 kHz without degrading the efficiency of the converter. In the multicellular converter, this frequency increase allows reducing the capacitance value of the flying capacitors. Nevertheless, in practice, the expected gain in weight and volume has to be nuanced, since the RMS current in the capacitor does not change with the switching frequency. Another gain, not developed in this paper, is the reduction of the output filtering elements. The output voltage waveform is also improved and therefore the quality of the harmonic spectrum [14].

If SiC components show advantages for the sizing of ICMCs, a special attention has to be paid in the 3-D design to reduce each loop inductance and insure safe commutations.

Furthermore, it is important to note that the control of multilevel converters is made possible by the evolution of FPGAs, which are more efficient and allow a high-frequency control of a large number of switches.

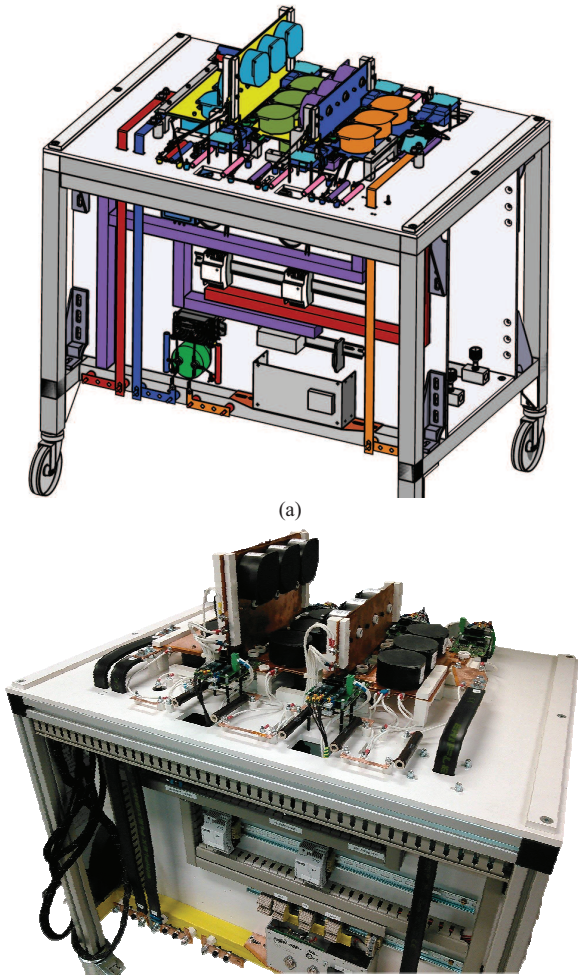

(a)

(b)

Fig. 12. ICMC with 1700 V / 300 A SiC-MOSFET HBMs - (a) final 3-D design, (b) picture of the real test-bench.

VI. Acknowledgment

This study is supported by the French National Research Agency (ANR), program on Sustainable Electricity Production and Management (PROGELEC).

References

[1] M. Debruyne, "High power IGBT traction drives", *WCRR'01; World Conference on Railway Research*, pp. 1-17, Cologne, Germany, November 2001.

[2] R. Hermann, E.U. Krafft, and A. Marz, "Reverse-conducting-IGBTs - A new IGBT technology setting new benchmarks in traction converters", *Power Electronics and Applications (EPE)*, 2013 15th European Conference on, pp. 1-8, Lille, France, Sept. 2013.

[3] J. Millan, "A review of WBG power semiconductor devices", *The International Semiconductor Conference (CAS)*, Vol. 1, pp.57-66, Oct. 2012.

[4] L. D. Stevanovic, K. S. Matocha, P. A. Losee, J. S. Glaser, J. J. Nasadoski, and S. D. Arthur, "Recent Advances in Silicon Carbide MOSFET Power Devices", *Applied Power Electronics Conference and Exposition (APEC)*, 2010 Twenty-Fifth Annual IEEE, pp. 401-407, February 2010.

[5] [Online]. (SiC Power Devices). Available: http://www.wolfspeed.com/

[6] S. Madhusoodhanan, K. Hatua, S. Bhattacharya, S. Leslie, Sei-Hyung Ryu, M. Das, A. Agarwal, and D. Grider, "Comparison study of 12kV n-type SiC IGBT with 10kV SiC MOSFET and 6.5 kV Si IGBT based on 3L-NPC VSC applications", *Energy Conversion Congress and Exposition (ECCE), 2012 IEEE*, pp. 310-317, Raleigh, N.C., Sept. 2012.

[7] C. Raynaud, D. Tournier, H. Morel, and D. Planson, "Comparison of high voltage and high temperature performances of wide bandgap semiconductors for vertical power devices", *Diamond & Related Materials*, Volume 19, Issue 1, pp. 1-6, January 2010.

[8] M. Mermet-Guyennet, A. Castellazzi, J. Fabre, and P. Ladoux, "Electrical Analysis and Packaging Solutions for High-Current Fast-Switching SiC Components", *Integrated Power Electronics Systems (CIPS), 2012 7th International Conference on,* Nuremberg, Germany, pp. 1-6, 6-8 March 2012.

[9] P. Ladoux, M. Mermet-Guyennet, J. Casarin, and J. Fabre, "Outlook for SiC devices in Traction Converters", ESARS'12, *IEEE International conference on Electrical Systems for Aircraft, Railway and Ship propulsion*, Bologna, Italy, pp. 1-6, 16-18 October 2012.

[10] S. Bernet, "Recent developments of high power converters for industry and traction applications", *Power Electronics, IEEE Transactions on*, vol. 15, Issue 6, pp. 1102-1117, November 2000.

[11] J. Fabre, P. Ladoux, and M. Piton, "Opposition Method based test bench for characterization of SiC Dual MOSFET Modules", *PCIM Europe 2013, International Exhibition and Conference for Power Electronics, Intelligent Motion, Renewable Energy and Energy Management; Proceedings of*, Nuremberg, Germany, pp. 998-1005, 14-16 May 2013.

[12] J. Fabre, P. Ladoux, and M. Piton, "Characterization and Implementation of Dual-SiC MOSFET Modules for future use in Traction Converters", *Power Electronics, IEEE Transactions on* , vol. 30, no. 8, pp. 4079-4090, August 2015.

[13] T.A. Meynard and H. Foch, "Multilevel choppers for high voltage applications," EPE Journal, vol. 2, no. 1, pp. 45–50, Mars 1992.

[14] F. Hamma, T.A. Meynard, F. Tourkhani, and P.Viarouge, "Characteristics and design of multilevel choppers", Power Electronics Specialists Conference, 1995. PESC '95 Record., 26th Annual IEEE (Volume:2), Atlanta, GA, 18-22 Jun 1995.

[15] T.A. Meynard, M. Fadel and N. Aouda, "Modeling of multilevel converters," in *IEEE Transactions on Industrial Electronics*, vol. 44, no. 3, pp. 356-364, June 1997.

[16] R.H. Wilkinson, T.A. Meynard and H.T. Mouton, "Voltage unbalance in the multicell converter topology," *6th IEEE AFRICON Conference in Africa*, vol. 2, pp. 759-764, October 2002.

[17] R.H. Wilkinson, H.T. Mouton and T.A. Meynard, "Stability analysis of multicell converters," *7th IEEE AFRICON Conference in Africa*, 2004, vol. 2, pp. 1131-1136, September 2004.

[18] C. Chen, X. Pei, Y. Chen, and Y. Kang, "Investigation, Evaluation, and Optimization of Stray Inductance in Laminated Busbar", *Power Electronics, IEEE Transactions on*, vol. 29, no. 7, pp. 3679-3693, July 2014.

[19] E. Batista, and J.M. Dienot, "EMC Characterization for Switching Noise Investigation on Power Transistors", *Electromagnetic Compatibility, 2008. EMC 2008. IEEE International Symposium on*, Detroit, Michigan, pp. 1-7, 18-22 August 2008.

[20] E. Batista, J.M. Dienot, M. Mermet-Guyennet, A. Castellazzi, "Accurate mixed electrical and electromagnetic model of a 6,5kV IGBT module", Power Electronics, 2007. ICPE'07. 7th Internatonal Conference on. IEEE, pp. 1151-1155, 2007.

[21] [Online]. (ANSYS Software). Available: http://www.ansys.com/

[22] [Online]. (AVX company) Available: http://www.avx.com/products/film-capacitors /medium-power-film-caps/ffvs-rohs-compliant/

[23] [Online]. (Siebel company) Available: http://www.siebel-elektronik.de/ downloads/Datenblatt-SW25-25.pdf

[24] [Online]. (LEM company) Available: http://www.lem.com/docs/marketing/LEM%20DV%20Leaflet%209_9_08.pdf